Optical Materials 90 (2019) 139–144

Contents lists available at ScienceDirect

Optical Materials

journal homepage: www.elsevier.com/locate/optmat

Optical, vibrational and fluorescence recombination pathway properties of nano SiO_2-PVA composite films

B. Karthikeyan[a,*], S. Hariharan[a], Arya Sasidharan[a], V. Gayathri[a], T. Arun[b], Ali Akbari-Fakhrabadi[b], C. Madhumitha[a]

[a] Nanophotonics Laboratory, Department of Physics, National Institute of Technology, Tiruchirappalli, Tamil Nadu, 620015, India
[b] Department of Mechanical Engineering, University of Chile, Santiago, 837045, Chile

ARTICLE INFO

Keywords:
Polymer nanocomposites
Amorphous silica
Poly vinylalcohol
Freestanding films
Optical properties

ABSTARCT

We report optical and spectroscopic investigations on polyvinyl alcohol (PVA)/silica composite free standing films. Amorphous silica nanoparticles are synthesized from rice husk ash using pyrolysis technique. PVA/silica nano composite free standing films are prepared by simple chemical method. As prepared nano composites are characterized using X-ray diffraction (XRD), field emission scanning electron microscopy (FESEM), transmission electron microscopy (TEM), diffuse reflectance spectroscopy (DRS), Fourier transform infrared spectroscopy (FTIR), Raman spectroscopy, photoluminescence spectroscopy (PL) and time resolved photoluminescence (TRPL) spectroscopy techniques. Spectroscopic studies reveal the structural modification of silica nanoparticle in PVA matrix due to the formation some new chemical bonds. The prepared PVA/Silica composites exhibit exceptional optical properties which can be applicable for Opto-electronic device applications.

1. Introduction

Silica nanoparticles are extensively used because of its optical absorption, emission properties, high surface to volume ratio and high reflectivity. Silica exist both in crystalline as well as amorphous forms. Amorphous silica attracted current research areas because of its exceptional optical properties [1]. Production of amorphous silica from rice husk ash find an environmental friendly method and it reduce the amount of biomass waste from paddy fields [2]. Calcination of rice husk leads to the formation of silica and it is the temperature that determines the nature of formed silica. High calcination temperature results crystalline silica. Temperature of the order of 800 °C is suitable for the formation of amorphous silica nanoparticle.

Polymer nanocomposites have gained significant interest because of its applications in Opto-electronics field [3–5]. They are widely applied for light emission technology [6,7]. Poly (vinyl alcohol) (PVA) is widely used because of its film forming properties, high hydrophilicity and biocompatibility. Only PEG/Silica and PMMA/silica nanocomposites are studied until now [8,9]. Also polymer modification of silica sol is studied mainly. Most of these works are concentrated on the mechanical properties of the polymer/silica nanocomposites. Optical properties of these kinds of nanocomposites are discussed rarely. In this work we are focusing mainly on the optical properties of the PVA/Silica nanocomposites. One of the significance of PVA/silica polymer is that it combines unique properties of inorganic fillers (Silica) including thermal, optical and mechanical property with that of organic polymer matrix (PVA) like process ability, biocompatibility, ductility etc. Spherical silica particle, silica nanotubes, layered silicates are used as organic fillers in polymer/silica nano composites [10–12]. Among these spherical silica nanoparticles are used widely because of their high surface volume ratio, ordered structure and ease of surface modification. In the present work, we study the optical and spectroscopic properties of PVA/silica nano composites using various spectroscopic techniques.

2. Experimental details

2.1. Materials

PVA was purchased from Sigma- Aldrich, HCl purchased from Merck Life Science Pvt. limited, Rice husk collected from a rice mill in Trichy. Double Distilled water was used throughout the experiment.

2.2. Preparation of SiO_2 from rice husk

15 g of rice husk were refluxed with 225 ml of 10 wt% HCl solution

* Corresponding author.
E-mail address: bkarthik@nitt.edu (B. Karthikeyan).

https://doi.org/10.1016/j.optmat.2019.01.063
Received 8 January 2019; Accepted 27 January 2019
Available online 07 March 2019

for 2 h in a round bottom flask. Then the acid leached rice husk were filtered out and rinsed with distilled water. This filtered husk were dried in a heating mantle at 100 °C for 4 Hrs. The rice husk ash formed was transferred into a crucible and placed in a muffle furnace. Ash is kept inside the furnace at 700 °C for 2 h. Formed white colored ash is grinded using pestle and mortar to get fine silica nanoparticle.

2.3. Preparation of PVA/SiO_2 nanocomposites

1 g of Poly (Vinyl) alcohol (PVA) is dispersed in 20 ml of double distilled water. It is then heated at 60 °C in a heating mantle until the PVA get completely dissolve in water. Four set of equal amount of above solution is taken and each is mixed with 0.025 g, 0.05 g, 0.075 g of synthesized silica respectively. After ultra-sonication, PVA-SiO_2 mixture is poured into a petri dish and allowed to dry under room temperature. After it get completely dry, free standing film of PVA-SiO_2 is peel off from petri dish. Thus PVA/SiO_2 composites were prepared. The prepared free standing films are name coded as S, P, PS1, PS2 and PS3 which represent pure silica, pure PVA film, and different quantities (0.025 g, 0.05 g, 0.075 g) of silica loaded PVA films respectively.

2.4. Instrumentation

Structure of the prepared SiO_2 sample and PVA/SiO_2 nanocomposites were studied using Rigaku Ultima III X-Ray Diffractometer with Cu-Kα as radiation source with a wavelength of λ = 1.54 Å. SEM analysis were carried out to study the surface morphology and particle size of silica nanoparticles. Different vibrational frequencies and corresponding chemical bonds were analyzed using Fourier Transform Infrared Spectroscopy (FTIR). FTIR spectra were recorded in the range 400–40000 cm^{-1}. Optical properties of the synthesized silica particles are investigated by recording absorption spectra in the range of 200–1000 nm using Jasco V-670 UV–Vis spectrometer. Vibrational properties are studied by recording Raman spectra using Lab-RAM HR Evolution Raman spectrometer with an excitation wavelength of 532 nm. PL studies were done using Horiba Jobin Yvon Fluoromax-4 system. TRPL studies were carried out using Horiba Jobin Yvon-Deltaflex TCSPC system.

3. Results and discussion

3.1. X-ray diffraction

XRD studies were carried out in 2θ range of 10 to 80° with a step size of 0.02° and it is shown in Fig. 1. Broad peak ranging from 15° to 30° centered at 22.3^0 is shown in the case of synthesized silica nanoparticle. This confirms the presence of SiO_2 in disordered crystobalite form (according to JCPDS reference number 89–3606 which corresponds to the (101) cubic crystalline plane of SiO_2.) The absence of sharp crystalline peaks shows that the SiO_2 nanoparticles are amorphous. The purity of synthesized silica was confirmed by the absence of sharp peaks corresponding to the any other metal ions. The characteristic diffraction peak of pure PVA is observed at about $2\theta = 19.46^0$ and a peak of low intensity is observed at 40.4^0. Former one corresponds to (101) plane of semi crystalline PVA while the later one represents the diffraction from (111) plane. Incorporation of SiO_2 into PVA matrix reduces the crystallinity of PVA. The XRD patterns of the PVA/SiO_2 composite shows broad peaks similar to that of the SiO_2. But it is broader than that of silica and centered around 22^0. With increasing the concentration of silica the peak become more flat. There is no significant change in the intensity of peak with change in concentration of SiO_2. Broader peak in the composite indicate they are amorphous. For pure PVA fiber, the crystallinity was high due to the hydroxyl groups in its side-chain. However, for PVA/SiO_2 composite, the hydroxyl groups of PVA molecules would react with silica; thus, the amounts of hydroxyl groups could be decreased, resulting in the decreasing of crystallinity

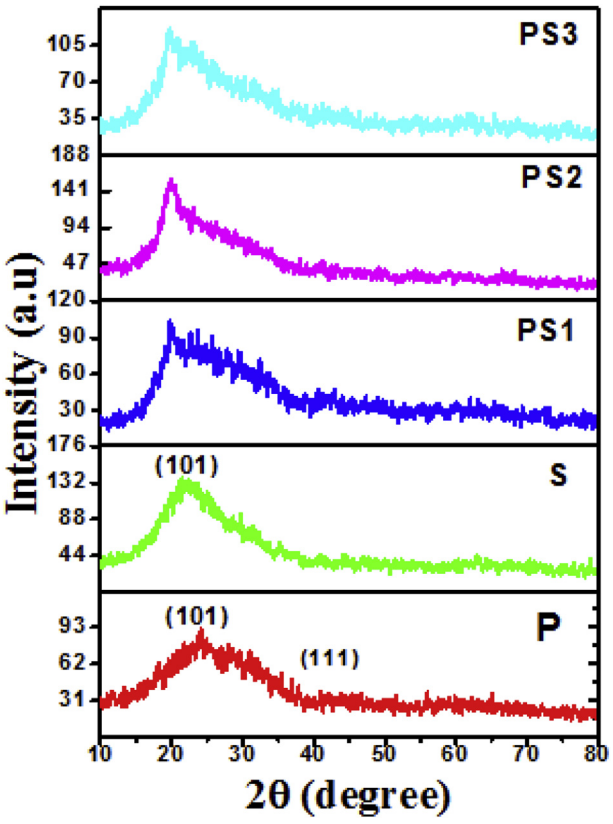

Fig. 1. XRD pattern of the PVA, SiO_2 and PVA/SiO_2 Composites.

[13].

3.2. Field emission scanning electron microscopy (FESEM) and transmission electron microscopy (TEM)

In order to study the surface morphology of the prepared SiO_2 samples were examined by FE-SEM, and the obtained image is shown in Fig. 2 (a). Image show that synthesized silica particles are nano structured with spherical morphology Aggregation of silica particle can be identified from FESEM micrographs. TEM image depicted in Fig. 2 (b) also show the formation of nano sized silica.

3.3. Diffuse reflectance and absorption spectroscopy

The reflectance measurements are carried out in the wavelength range 200–1100 nm. Fig. 3(a) shows the reflectance spectra of PVA/SiO_2 nanocomposites. Pure PVA film has reflectance around 90%. But as the concentration of silica in PVA polymer matrix increases, the reflectance decreases. Composite with high concentration of SiO_2 (PS3) has lowest reflectance.

This is because the PVA/SiO_2 composite become more and more amorphous as the concentration of silica in PVA matrix increases. Optical absorption spectra of PVA/SiO_2 nanocomposites are given in Fig. 3 (b). There is one strong absorption peak at 372 nm and weak one at 438 nm observed for pure silica (S). Thus silica particle have strong absorption in UV region and very little absorption in visible region. But in composites, all the peaks of silica are suppressed. Absorbance of the film increases with the increase of the SiO_2 concentration in the PVA polymer matrix.

3.4. Fourier Transform Infrared Spectroscopy

From the FTIR spectrum of SiO_2 nanoparticle (S) as shown in Fig. 4, presence of relatively strong bands at 462 cm^{-1}, 797 cm^{-1}, 1067 cm^{-1}

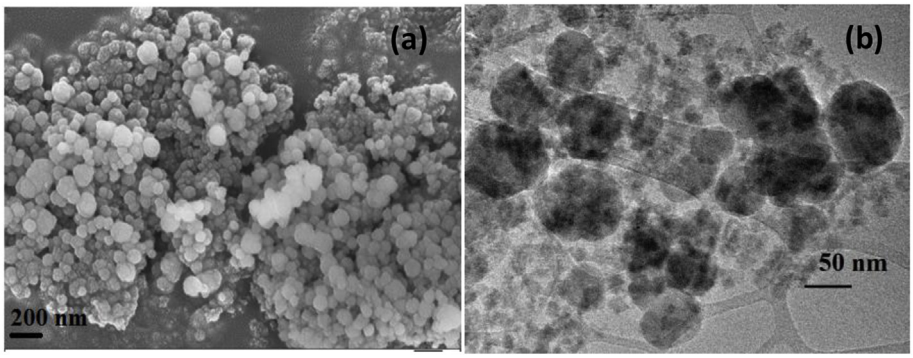

Fig. 2. (a) FESEM image of pure SiO_2 (b) TEM image of pure SiO_2.

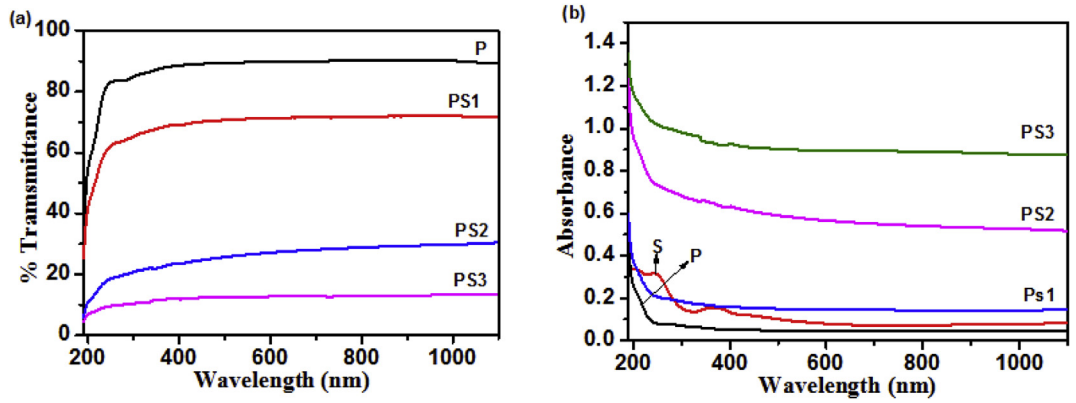

Fig. 3. (a) Transmittance spectra of the prepared composite films (b) Absorption spectra of the prepared composite films.

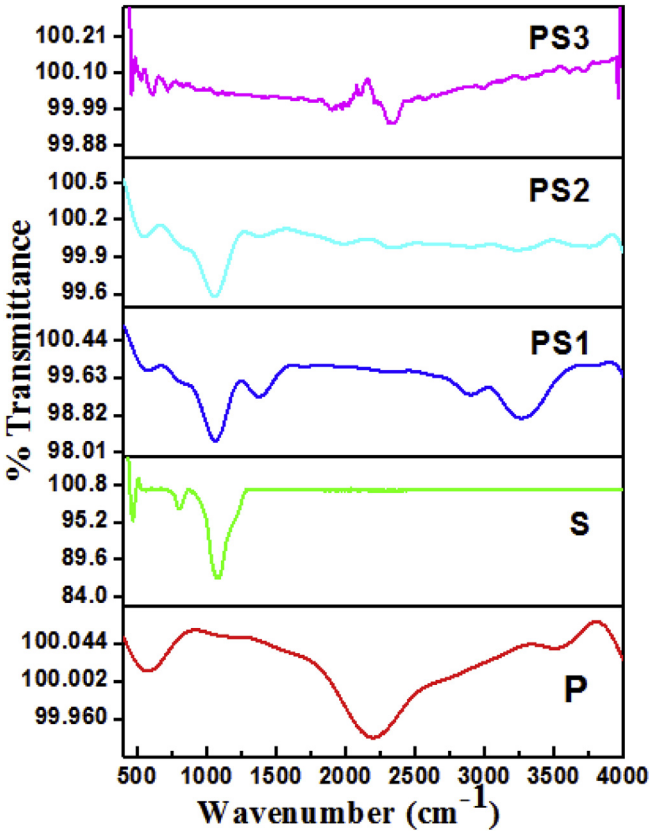

Fig. 4. FTIR spectra of the PVA, SiO_2 and PVA/SiO_2 Composite films.

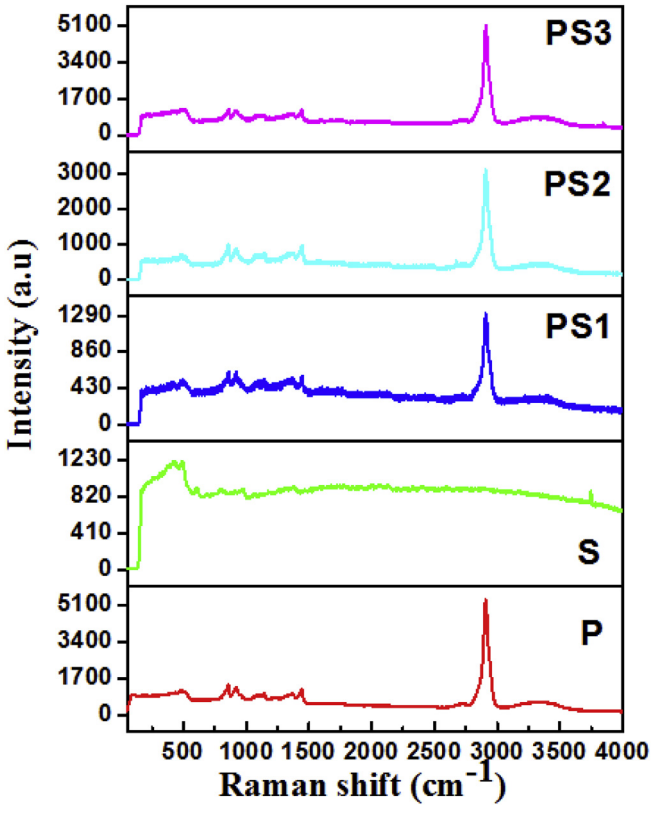

Fig. 5. Raman spectra of the PVA, SiO_2 and PVA/SiO_2 Composite films.

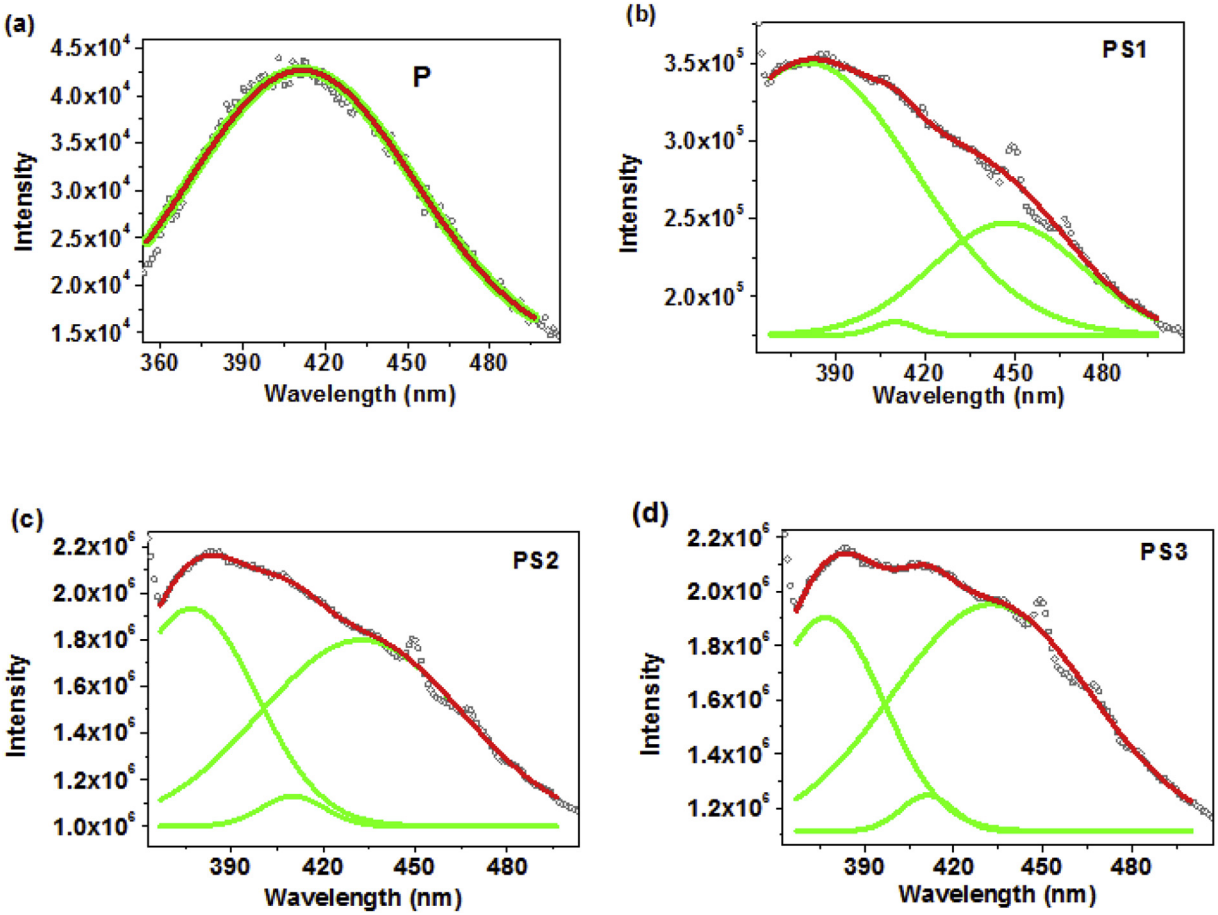

Fig. 6. PL spectra of pure PVA and Silica loaded PVA freestanding films. All samples were excited at 330 nm. The obtained spectra are Gaussian de-convoluted for analysis.

and weak band at 1235 cm^{-1} can be observed. Absorption peak at 462 cm^{-1} corresponds to Si—O rocking (bending) vibration while the peak at 797 cm^{-1} is due to Si—O symmetric stretching. The bands at 1067 cm^{-1} and weak band at 1235 cm^{-1} are due to Si—O—Si asymmetric stretching vibration. FTIR spectrum of pure PVA film (P) shows a strong hydroxyl band for free alcohol at 3538 cm^{-1}. This corresponds to the non-bonded —OH stretching of PVA molecule. This demonstrates that the strong intermolecular and intramolecular hydrogen bonding. One broader peak at 2207 cm^{-1} is due to C—C stretching while one at 1100 cm^{-1} is due to C—O stretching vibration. Bands in the range of 1370 cm^{-1} is attributed to the strong bending vibration of C—H bonds while that in 2800 cm^{-1} is the result of variable stretching vibration of C—H bond. From Fig. 4, it is observed that many new peaks are appeared when PVA/SiO_2 nanocomposite is formed. There is a broad band of order 3700-3800 cm^{-1} is present in the nanocomposites which is resulted from the free Si—OH stretching vibration and this may be due to incompleteness of the condensation of inorganic polymer network. But the bands present in the range of 3200-3400 cm^{-1} is due to hydrogen bonded Si—OH vibration. In the case of both PS1 and PS2, a sharp peak is present near 1060 cm^{-1}. This corresponds to the Si—O—C stretching vibrations which demonstrate that the organic phase is linked with inorganic phase through covalent bond. Bands present in the range of 2000-2150 cm^{-1} indicates the strong Si—H vibration.

3.5. Raman spectroscopy

From the Raman spectrum of SiO_2 (S) given in Fig. 5, with an excitation wavelength of 532 nm and power 50 mW,we can observe R band at 421 cm^{-1} and D band at 1352 cm^{-1} [14]. The D band is an indicator of disorder resulting from structural defects. R band represent the maximum of the distribution of the Si—O—Si angle. The band present at 820 cm^{-1} is due to the SiO—H vibration. For the pure PVA, the peak at 1440 cm^{-1} is ascribed to the stretching vibration of C—H bond in the PVA molecules, and the most intense band centered at 2911 cm^{-1} is assigned to the stretching vibrations of $-CH_2$. Peaks at 853 cm^{-1} and 917 cm^{-1} are related to C—C stretching vibration. In the Raman spectra of PVA/SiO_2 nanocomposite, characteristic peak of only PVA is present. All the three peaks of PVA is preserved in the composite. The characteristic peak of silica at 421 cm^{-1} is suppressed in the composite.

3.6. Photoluminescence spectroscopy

The PL spectra of prepared composite freestanding films under excitation at 330 nm are depicted in Fig. 6. Fig. 6 (a) shows the PL spectrum of pure PVA. The pure PVA show broad PL emission band in the region 360–480 nm with emission peak centered at 410 nm. The emission of PVA is attributed to the LUMO-HOMO transitions. Silica loaded samples show broad PL emission covering the UV, blue and blue-green regions. Generally the PL characteristic of silica depends on its environment. The PL of silica arise due to the neutral oxygen vacancy and intrinsic defect centers [15,16]. The emission spectra of silica loaded samples show broad emission with three distinct bands centered at 385, 410 and 445 nm. The obtained bands are attributed to the characteristic emission of silica. The obtained emission spectra are Gaussian de-convoluted. Moreover the obtained bands are clearly matches with the band gap transitions of silica. It is observed that varying the weight percentage of silica did not significantly alter the

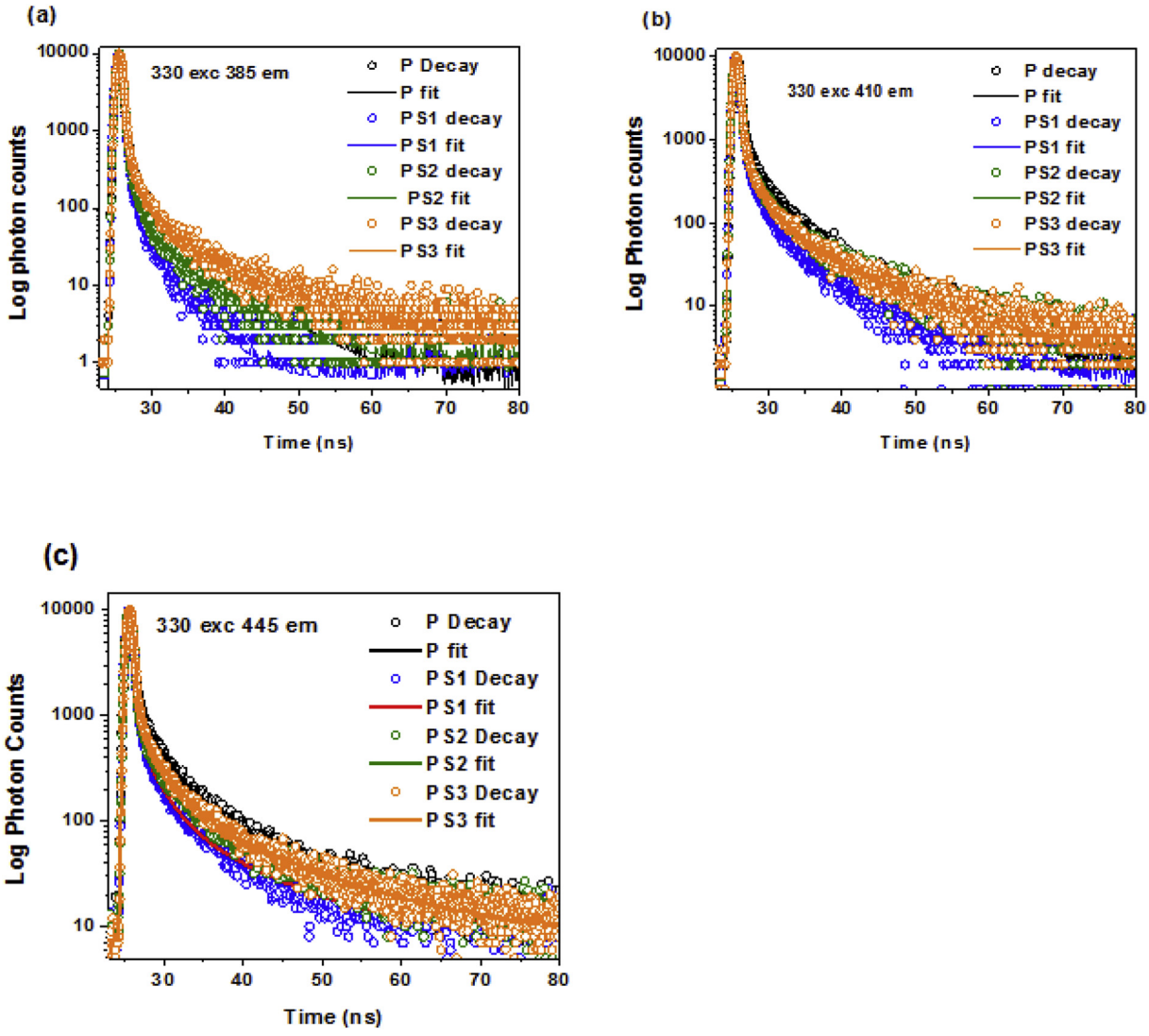

Fig. 7. Time resolved PL spectra of pure PVA and Silica loaded PVA freestanding films. All samples were excited at 330 nm. The emission decay dynamics was studied at three different wavelengths 385, 410 and 445 nm. The obtained spectra are fitted by triple exponential decay equation.

Table 1
Fit parameters for TRPL spectra depicted in Fig. 7 (a).

	A	B_1	B_2	B_3	T_1 (s)	T_2 (s)	T_3 (s)	Tavg (ns)
P	0.2847021	90.13	5.85	4.03	1.304382E-10	2.193271E-09	7.299684E-09	4.5258
PS1	0.6222714	−7504.58	7600.42	4.16	8.527254E-11	8.67257E-11	3.364364E-09	1.49591
PS2	0.6542218	94.19	3.73	2.08	1.136346E-10	2.347601E-09	8.824412E-09	4.85906
PS3	0.9516299	89.19	6.55	4.26	1.212701E-10	2.442425E-09	1.112205E-08	7.64682

Table 2
Fit parameters for TRPL spectra depicted in Fig. 7 (b).

	A	B_1	B_2	B_3	T_1 (S)	T_2 (S)	T_3 (S)	Tavg (ns)
P	1.064589	14.01	75.40	10.59	2.324576E-09	1.307723E-10	8.668962E-09	6.5025
PS1	0.8998663	7.99	86.89	5.12	2.206821E-09	1.258909E-10	8.310827E-09	5.5387
PS2	1.316942	9.73	7.60	82.67	2.59234E-09	1.093126E-08	1.144814E-10	8.27591
PS3	1.363248	9.93	83.11	6.96	2.679398E-09	1.122339E-10	1.170626E-08	8.73957

emission at 385 and 410 nm region. But the emission band at 445 nm is observed to be increases with increasing the loading amount of silica in PVA matrix. There is no shift in the emission wavelength observed with increasing the loading amount of silica in the PVA matrix. The PL of silica is preserved in the PVA matrix.

3.7. Time resolved photoluminescence spectroscopy

Time resolved photoluminescence (TRPL) spectra of the prepared composite freestanding films are shown in Fig. 7. The prepared films are excited at 330 nm using ns diode laser with the repletion rate of

Table 3
Fit parameters for TRPL spectra depicted in Fig. 7 (c).

	A	B_1	B_2	B_3	T_1 (S)	T_2 (S)	T_3 (S)	Tavg (ns)
P	10.92623	19.25	66.20	14.55	2.676101E-09	1.223059E-10	1.103248E-08	8.67567
PS1	9.11156	9.57	82.69	7.74	2.205162E-09	9.959451E-11	9.289169E-09	7.06491
PS2	8.882573	12.54	77.63	9.82	2.900906E-09	1.116152E-10	1.315045E-08	10.3612
PS3	7.469073	14.74	11.56	73.71	2.667934E-09	1.272993E-08	1.089098E-10	10.1748

1 MHz. The emission decay dynamics is measured using time correlated single photon counting method. The excitation wavelength is fixed at 330 nm and the emission decay dynamics is studied at three different wavelengths 385, 410 and 445 nm where we observed three emission bands in steady sate PL spectra. The emission decay dynamics of the films at 385 emission wavelength are shown in Fig. 7(a). The obtained emission decay dynamics are fitted by exponential equation given by $y(x) = A + \sum_i^n B_i exp\left(\frac{-x}{\tau_i}\right)$ where, n is the number of discrete emissive species, A is a baseline correction usually called as "dc" offset. B_i is the pre exponential factor and τ_i is the excited-state fluorescence lifetime associated with the ith component. The fitted parameters are given in Table 1. The average lifetime is calculated using the equation $t_{avg} = \sum_i f_i\, t_i$, where $f_i = \frac{\alpha_i t_i}{\sum_i \alpha_i t_i}$. The obtained parameters show that the pre exponential factors and lifetime components have considerable variations with increasing the loading amount of silica in PVA matrix. The average lifetime for the pure PVA is found to be 4.52 ns. For the highest amount of silica loaded film, the average lifetime is found to be 7.64 ns. This shows that the average lifetime increases with increasing the loading amount of silica in the PVA matrix. This lifetime enhancement shows the long lived electrons in the excited stated due to the strong interaction between the silanol groups in silica and hydroxyl groups in the PVA. Similar kind of result is found for the decay dynamics at 410 nm emission wavelength. Here, the average lifetime of PVA is found to be 6.5 ns. For the highest quantity of silica loaded film, the average lifetime is found to be 8.74 ns. The decay dynamics at 445 nm emission wavelength also show enhanced average lifetime. The average lifetime of the pure PVA is calculated to be 8.67 ns, which is found to be increased to 10.17 ns for the highest amount of silica loaded film (see Tables 2 and 3).

4. Conclusion

Spectroscopic investigations were done on silica derived from rice husk and PVA/silica composite free standing films. XRD pattern of the prepared composites showed that the crystallinity of PVA losses when silica is added to PVA matrix. The reflectivity of the composite decreases with increasing the loading amount of silica. Absorption peaks of SiO_2 were suppressed by PVA in the composites. Structural modification due to the formation of new bonds in composites was confirmed from the FTIR and Raman spectroscopy studies. Thus, the grafting of silica in PVA matrix resulted in the surface modification of silica particle. PL and TRPL results showed that the characteristic emission of silica is preserved in the PVA matrix and also the enhanced average life time was observed in the composite films which showed the long lived electrons in the excited state as a result of interaction between the silanol groups of silica and hydroxyl groups of PVA. PVA/Silica composite showed exceptional optical properties which could be suitable for Opto-electronic applications.

References

[1] D. Ren, B. Xiang, C. Hu, K. Qian, X. Cheng, The electronic and optical properties of amorphous silica with hydrogen defects by ab initio calculations, J. Semiconduct. 39 (2018) 042002.
[2] S. Chandrasekhar, K.G. Satyanarayana, P.N. Pramada, P. Raghavan, T.N. Gupta, Review Processing, properties and applications of reactive silica from rice husk—an overview, J. Mater. Sci. 38 (2003) 3159–3168.
[3] T. Nguyen, Polymer-based nanocomposites for organic optoelectronic devices: a review, Surf. Coating. Technol. 206 (2011) 742–752.
[4] S. Li, M.M. Lin, M.S. Toprak, D.K. Kim, M. Muhammed, Nanocomposites of polymer and inorganic nanoparticles for optical and magnetic applications, Nano Rev. 1 (2010) 5214.
[5] J. Ouyang, C.W. Chu, F.C. Chen, Q. Xu, Y. Yang, High-conductivity poly(3,4-ethylenedioxythiophene):poly(styrene sulfonate) film and its application in polymer optoelectronic devices, Adv. Funct. Mater. 15 (2005) 203–208.
[6] K. Gipson, B. Ellerbrock, K. Stevens, P. Brown, J. Ballato, Light-emitting polymer nanocomposites, J. Nanotech. (2011) 1–8.
[7] J. Lee, V.C. Sundar, J.R. Heine, M.G. Bawendi, K.F. Jensen, Full color emission from II–VI semiconductor quantum dot–polymer composites, Adv. Mater. 12 (2000) 1102–1105.
[8] S.Y. Kim, H.W. Meyer, K. Saalwächter, C.F. Zukoski, Polymer dynamics in PEG-silica nanocomposites: effects of polymer molecular weight, temperature and solvent dilution, Macromolecules 45 (2012) 4225–4237.
[9] F. Zhang, D. Lee, T.J. Pinnavaia, PMMA/mesoporous silica nanocomposites: effect of framework structure and pore size on thermomechanical properties, Polym. Chem. 1 (2010) 107–113.
[10] F. Dalmas, N. Genevaz, M. Roth, J. Jestin, E. Leroy, 3D dispersion of spherical silica nanoparticles in polymer nanocomposites: a quantitative study by electron tomography, Macromolecules 47 (2014) 2044–2051.
[11] Z. Yu, X. Wang, Q. Su, J. Shan, J. Zheng, The effect of silica nanotubes on mechanical performance of polymethyl methacrylate nanocomposites: comparison to spherical nano-silica, J. Reinforc. Plast. Compos. 34 (2015) 1433–1443.
[12] S. Pavlidoua, C.D. Papaspyrides, A review on polymer–layered silicate nanocomposites, Prog. Polym. Sci. 33 (2008) 1119–1198.
[13] H. Ma, T. Shi, Q. Song, Synthesis and characterization of novel PVA/SiO_2-TiO_2 hybrid fibers, Fibers 2 (2014) 275–284.
[14] A. Alessi, S. Agnello, G. Buscarino, F.M. Gelardi, Raman and IR investigation of silica nanoparticles structure, J. Non-Cryst. Solids 362 (2013) 20–24.
[15] Yunliang Yue, Yu Song, Xu Zuo, First principles study of oxygen vacancy defects in amorphous SiO2, AIP Adv. 7 (2017) 015309.
[16] C.L. Kuo, S. Lee, G.S. Hwang, Strain-induced formation of surface defects in amorphous silica: a theoretical prediction, Phys. Rev. Lett. 100 (2008) 076104.